

Forward-Backward Multiplicity Correlations in $\sqrt{s_{NN}} = 200$ GeV Au+Au Collisions

B.B.Back¹, M.D.Baker², M.Ballintijn⁴, D.S.Barton², R.R.Betts⁶, A.A.Bickley⁷, R.Bindel⁷, A.Budzanowski³, W.Busza⁴, A.Carroll², Z.Chai², M.P.Decowski⁴, E.García⁶, T.Gburek³, N.George^{1,2}, K.Gulbrandsen⁴, S.Gushue², C.Halliwell⁶, J.Hamblen⁸, M.Hauer², G.A.Heintzelman², C.Henderson⁴, D.J.Hofman⁶, R.S.Hollis⁶, R.Holyński³, B.Holzman², A.Iordanova⁶, E.Johnson⁸, J.L.Kane⁴, J.Katzy^{4,6}, N.Khan⁸, W.Kucewicz⁶, P.Kulinich⁴, C.M.Kuo⁵, W.T.Lin⁵, S.Manly⁸, D.McLeod⁶, A.C.Mignerey⁷, R.Nouicer⁶, A.Olszewski³, R.Pak², I.C.Park⁸, H.Pernegger⁴, C.Reed⁴, L.P.Remsberg², M.Reuter⁶, C.Roland⁴, G.Roland⁴, L.Rosenberg⁴, J.Sagerer⁶, P.Sarin⁴, P.Sawicki³, H.Seals², I.Sedykh², W.Skulski⁸, C.E.Smith⁶, M.A.Stankiewicz², P.Steinberg², G.S.F.Stephans⁴, A.Sukhanov², J.-L.Tang⁵, M.B.Tonjes⁷, A.Trzupek³, C.Vale⁴, G.J.van Nieuwenhuizen⁴, S.S.Vaurnovich⁴, R.Verdier⁴, G.I.Verés⁴, E.Wenger⁴, F.L.H.Wolfs⁸, B.Wosiek³, K.Woźniak³, A.H.Wuosmaa¹, B.Wysłouch⁴

¹ Argonne National Laboratory, Argonne, IL 60439-4843, USA

² Brookhaven National Laboratory, Upton, NY 11973-5000, USA

³ Institute of Nuclear Physics PAN, Kraków, Poland

⁴ Massachusetts Institute of Technology, Cambridge, MA 02139-4307, USA

⁵ National Central University, Chung-Li, Taiwan

⁶ University of Illinois at Chicago, Chicago, IL 60607-7059, USA

⁷ University of Maryland, College Park, MD 20742, USA

⁸ University of Rochester, Rochester, NY 14627, USA

(Dated: November 16, 2018)

Forward-backward correlations of charged-particle multiplicities in symmetric bins in pseudorapidity are studied in order to gain insight into the underlying correlation structure of particle production in Au+Au collisions. The PHOBOS detector is used to measure integrated multiplicities in bins centered at η , defined within $|\eta| < 3$, and covering intervals $\Delta\eta$. The variance σ_C^2 of a suitably defined forward-backward asymmetry variable C is calculated as a function of η , $\Delta\eta$, and centrality. It is found to be sensitive to short range correlations, and the concept of “clustering” is used to interpret comparisons to phenomenological models.

PACS numbers: 25.75.Dw

At the top energies reached for Au+Au collisions at the Relativistic Heavy Ion Collider ($\sqrt{s_{NN}} = 200$ GeV), most of the energy is carried by particles with large longitudinal momenta. In general, these momenta are best expressed with the rapidity variable ($y = \frac{1}{2} \ln \frac{E+p_z}{E-p_z}$) or its near equivalent, the pseudorapidity variable ($\eta = -\ln(\tan(\theta/2))$). In strongly interacting systems, it is often thought that correlations between two particles are mainly “short-range” in rapidity. Indeed, short range correlations have been observed in pp and $\bar{p}p$ collisions over a wide range of beam energies [1] via two-particle correlation measurements. However, they have never been shown to be the only source of correlation in multiparticle production.

Indeed, single-particle rapidity (or pseudorapidity) distributions for inclusive charged particles produced in heavy ion collisions reveal a distinct “trapezoidal” structure stretching across the full rapidity range available in these reactions. More importantly, there is no evidence for an extended boost invariance, which would imply independent emission from different rapidity regions. Rather, two non-trivial effects are visible in the centrality dependence of particle production, which are apparently long-range in rapidity. The first is the fact that integrating over the full phase space reveals that particle production depends linearly on the number of

participants [2]. The second is that this occurs despite a significant change in the shape of the pseudorapidity dependence as a function of centrality, which happens to be collision-energy independent in the forward region [3].

All of this suggests that charged-particle production is highly correlated over large regions of rapidity, which naturally begs the question of the underlying structure of the single-particle distributions. In this paper, we discuss how to take first steps in this direction via the study of forward-backward multiplicity correlations. By this is meant the event-by-event comparison of the integrated multiplicity N_F in a bin defined in the forward ($\eta > 0$) region, centered at η with pseudorapidity interval $\Delta\eta$, with the multiplicity N_B measured in an identical bin defined in the backward hemisphere, centered at $-\eta$. With these definitions, one can construct the event-wise observable $C = (N_F - N_B)/\sqrt{N_F + N_B}$, and measure the variance σ_C^2 for a set of events with nominally similar characteristics (e.g. collision centrality).

The C variable is chosen to have particular sensitivity to various types of long and short range correlations. An “intrinsic” long-range correlation [4] in the emission of particles into the forward *and* backward hemisphere from a single source would give $N_F - N_B = 0$ with a substantial value of $N_F + N_B$, forcing C to 0. However, if the particle sources tended to produce into the forward *or* back-

ward region, such that the partitioning was binomial, this would lead to $\sigma_C^2 = 1$, since $\sigma^2(N_F - N_B) = N_F + N_B$ in that case. Direct studies of $\langle N_F \rangle$ as a function of N_B were used by UA5 for $\bar{p}p$ collisions to conclude that there are no large intrinsic correlations in particle production. And yet, a non-trivial long range correlation between the hemispheres persists, even when excluding the central two units of pseudorapidity [1, 4].

Short-range correlations would arise if objects emitted into either hemisphere break into $\langle k \rangle$ particles on average, with a variance of σ_k^2 , each of which remains close in rapidity (e.g. due to isotropic emission). Such intrinsic short-range correlations have in fact been measured in $\bar{p}p$ and pp experiments by direct construction of the two-particle correlation function in η . In a series of papers, the UA5 collaboration explored the hypothesis that particle emission was dominated by the decay of “clusters” locally in rapidity space [1, 4]. By varying $\Delta\eta$ and measuring the ratio $4\sigma_F^2/\langle N_F \rangle$ as a function of $N_F + N_B$, they found an “effective” cluster multiplicity ($k_{eff} = \langle k \rangle + \sigma_k^2/\langle k \rangle$) of approximately 2 charged particles. This exceeds the multiplicity expected from a resonance gas using masses up to 1.5 GeV, which gives an average multiplicity per particle of about $\langle k \rangle \sim 1.5$ [5], suggesting that clusters may have a variety of dynamical sources (although, to be sure of this, resonances over a wider mass range than in the previous calculations should be taken into account).

The decay of clusters has a particular effect on σ_C^2 . Consider the idealized case, where a cluster decays into exactly k particles, and all of the N particles are randomly distributed into identical η -bins in the forward or backward directions. In this case, the underlying fluctuations are those associated with N/k objects rather than N independent particles, and $C \rightarrow \sqrt{k}C$. In other words, σ_C^2 is linear with the cluster multiplicity for this simple case. In a more realistic physical situation, particles from each cluster may fall outside the chosen η -bin, or even in the opposite hemisphere. This results in a non-trivial modification of the measured value of k , but one which is still related directly to k , or rather k_{eff} (which incorporates the effect of the multiplicity per cluster having its own distribution). This relationship can be explored with the use of simulations and thus used to extract the effective cluster multiplicity with measured forward-backward correlations. These studies show that forward-backward correlations have the surprising ability to measure a fundamental *local* property of particle production.

The data analyzed here were taken with the PHOBOS detector [6] during Runs 2 and 4, in 2001 and 2004, respectively. The pseudorapidity acceptance was restricted to that of the “Octagon” detector, which is a tube of silicon sensors covering $|\eta| < 3$ and full azimuth except for a region near midrapidity. To simplify the analysis for different values of η and $\Delta\eta$, only the regions of the detector with complete rapidity coverage were kept, restrict-

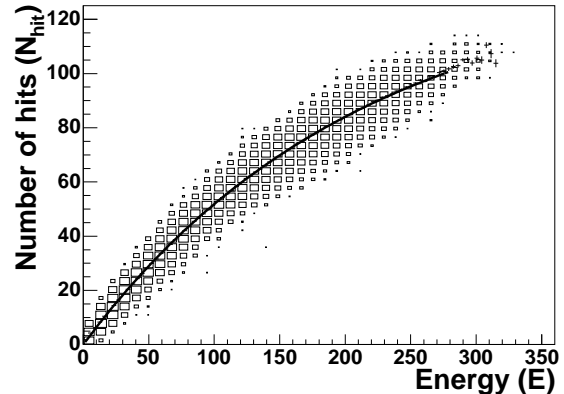


FIG. 1: Number of hits vs. total deposited energy (in keV) measured $-0.5 < \eta < 0$ (in the Octagon detector) for 200 GeV Au+Au collisions. The solid line is a function, described in the text, fit to the mean number of hits in each energy bin.

ing the total azimuthal acceptance to $\Delta\phi = \pi$, in four 45-degree wedges [7]. The multiplicity in each bin is estimated event-by-event by summing up the angle-corrected deposited energy of all hits and then dividing by the average energy per particle [8]. The average is calculated by a fit to the distribution of $\langle N_{hits} \rangle$ vs. the total deposited energy (E), an example of which is shown in Fig. 1, with the function $\langle N_{hit} \rangle = N_{max}(1 - e^{-E/E_{max}})$. The average energy per particle is given by E_{max}/N_{max} . This removes nearly all occupancy-related effects. Beyond the usual lower threshold to define a hit in the silicon, an η -dependent upper bound of the deposited energy per hit is applied to reduce the effect of low-momentum secondaries on the fluctuations of the single-particle dE/dx distributions, while keeping 97% of the primaries. The average $\langle C \rangle$, calculated as a function of η , centrality, and event vertex, is subtracted event-by-event to correct for gaps in the Octagon. This correction was studied in detail with simulations, and was found to leave the fluctuations unaffected.

To provide information that can be compared directly to models, a procedure was developed to estimate and remove the detector effects from the raw measured value of σ_C^2 ($\sigma_{C,raw}^2$) by using Monte Carlo (MC) simulations of the PHOBOS apparatus. The basic idea is to assume that $\sigma_{C,raw}^2 = \sigma_C^2 + \sigma_{det}^2$, where σ_{det}^2 is the contribution from detector effects, and use the MC to subtract it on average, leaving behind only the correlations between primary particles. It is found that there are several sources which contribute differently as a function of η and combine in quadrature to a nearly-constant value over the pseudorapidity range covered by the Octagon [8], as illustrated in Fig. 2. Gaps between the silicon sensors tend to be most important near mid-rapidity and decrease rapidly with angle as the particle density de-

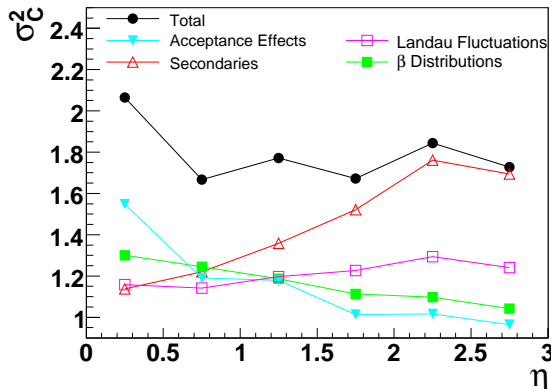


FIG. 2: Contributions to σ_C^2 from sources other than primary charged particles.

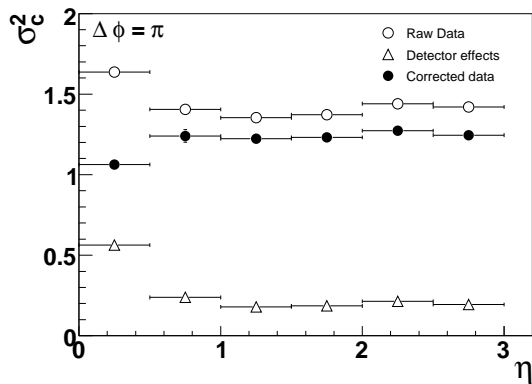


FIG. 3: Example of the analysis method, showing the raw values of σ_C^2 ($\sigma_{C,raw}^2$), the contribution from detector effects (σ_{det}^2 , as estimated using modified HIJING), and the subtracted result (σ_C^2) for bins of $\Delta\eta = 0.5$ as a function of η in the Run 4 data set. Note that these values are calculated for the half-azimuth ($\Delta\phi = \pi$) acceptance, which is corrected-for in the final result.

creases. Similarly, larger-angle particles tend to be slower than those at forward angles, leading to larger fluctuations in the energy deposition in the single layer of silicon. At the same time, the number of secondary particles emitted from primaries interacting in the beryllium beampipe rises quickly with increasing rapidity. This leads to increased fluctuations, even though some of the background is removed with a properly-chosen lower cut on the angle-corrected dE/dx of each hit. We have also studied fluctuations from the momentum (or β) distributions of the particles incident on the detector. In this case, the contribution to σ_C^2 decreases with increasing rapidity.

The detector effects are corrected on average by calcu-

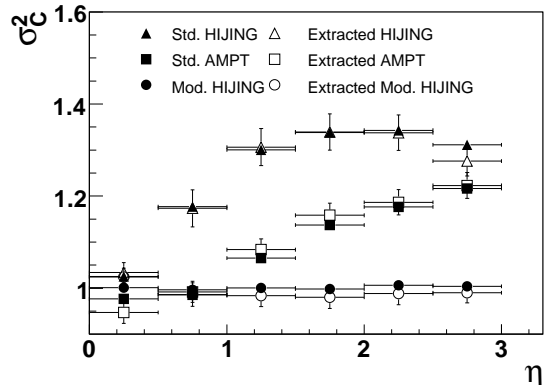


FIG. 4: Calibration of reconstruction method with MC simulations, as a function of η with $\Delta\eta = 0.5$. Solid points represent MC truth information on σ_C^2 , while the open symbols represent the outcome of the reconstruction procedure.

lating σ_C^2 using a modified HIJING simulation with all intrinsic correlations destroyed by flipping the sign of η at random, effectively breaking any rapidity-dependent multi-particle correlations and forcing $\sigma_C^2 = 1$. This allows a direct estimation of σ_{det}^2 . An example of this is shown in Fig. 3, which shows the raw values of σ_C^2 ($\sigma_{C,raw}^2$), the contribution from detector effects (σ_{det}^2 , as estimated from modified HIJING), and the subtracted result (σ_C^2) for bins of $\Delta\eta = 0.5$ as a function of η in the Run 4 data set. There is a small residual correlation of σ_{det}^2 with σ_C^2 , parametrized as $\sigma_{det}^2 = \sigma_{det,raw}^2 (1 - \alpha(\sigma_C^2 - 1))$, which is removed by estimation of α as a function of η , $\Delta\eta$ and centrality. Finally, we correct for using only half-azimuth acceptance by $\sigma_C^2 \rightarrow 2(\sigma_C^2 - 1) + 1$, a formula obtained using MC simulations, assuming that the limited acceptance only reduces the probability of measuring all of the particles in a typical cluster.

Systematic uncertainties were calculated by varying several variables involved the estimation of σ_C^2 (data sets, event generators, and dE/dx cuts) and found to be around $\Delta\sigma_C^2 \sim 0.1$. The bin-to-bin variation of the systematic error calculation was adjusted to reduce fluctuations from the error determination procedure.

After correcting for detector effects, the results on σ_C^2 can be directly compared with model calculations based on charged primary particles. We have focused mainly on HIJING [9] and AMPT [10] (which includes partonic and hadronic transport codes), both of which have been used to describe various features of heavy ion collisions at RHIC energies. Fig. 4 shows the results of the correction procedure described above on three simulations. Two of them are based on standard versions of HIJING and AMPT, and a third on the modified HIJING, as described previously. One sees that in all three cases, the reconstructed values of σ_C^2 , using the same tuning in all

cases, match the σ_C^2 extracted from the primary charged particles within statistical precision.

The first set of results concerns the η dependence of σ_C^2 , for forward and backward bins that are $\Delta\eta = 0.5$ units wide, as shown in the upper panel of Fig. 5. In this case, HIJING and AMPT already show some differences related to their underlying physics scenarios. For peripheral (40-60%) events, both models have a similar magnitude and a monotonically-rising η dependence. Central events show a substantial difference extending over most of the rapidity range, with AMPT showing a systematically smaller value of σ_C^2 . This may be due to the initially produced clusters being smeared out in rapidity space by the hadronic rescattering stage. Also, it is observed that both data and MC show $\sigma_C^2 \sim 1$ at $\eta = 0$. This is suggestive of the effect predicted by Jeon and Shi [11], that the formation of a QGP near mid-rapidity should break up any sort of cluster structure seen in pp and thus lead to a reduction in σ_C^2 . However, it can also be explained by the fact that clusters produced at $\eta = 0$ tend to emit particles into *both* the N_F and N_B side, inducing an “intrinsic” long-range correlation that decreases σ_C^2 . Simulations show that this effect is not modified by the precise values of $\langle k \rangle$ and σ_k^2 , for constant k_{eff} . In any case, the data are systematically higher than the model calculations for both peripheral and central events.

The next set of results is the $\Delta\eta$ dependence of σ_C^2 , with a fixed bin position $\eta = 2.0$, as shown in the lower panel of Fig. 5. One sees that for both peripheral and central data, σ_C^2 rises monotonically with increasing pseudorapidity interval. This can be explained as an acceptance effect in the context of cluster emission: by increasing $\Delta\eta$, one increases the probability of observing more than one particle emitted from a single cluster in either N_F or N_B . Clearly, the rate of change with $\Delta\eta$ should reflect the full cluster distribution (both $\langle k \rangle$ and σ_k), but these studies are not yet sufficiently precise to determine the detailed properties of clusters produced in RHIC collisions. It is striking that the peripheral data has already reached $\sigma_C^2 \sim 3$ for the largest $\Delta\eta$ while this number is closer to 2 for central data. Finally, it is interesting that neither HIJING nor AMPT can explain both the centrality and $\Delta\eta$ dependence simultaneously. AMPT never agrees with the data in magnitude, but at least predicts a larger σ_C^2 in peripheral events than in central events. This should be contrasted with HIJING, which reproduces the central data but has no centrality dependence at all, at odds with the experimental data.

In conclusion, measurements of forward-backward fluctuations of charged-particles produced in Au+Au collisions

at $\sqrt{s_{NN}} = 200$ GeV may provide insight into the structure of long and short range correlations in pseudorapidity space. Our data for 200 GeV Au+Au collisions are now fully corrected for detector and background effects, so direct comparisons can be made to phenomenological models. We see significant short-range correlations at all centralities and pseudorapidities, instead of just at mid-rapidity. There is a non-trivial centrality and rapidity dependence of these correlations, in both η and $\Delta\eta$. Finally, neither HIJING nor AMPT reproduces all of the main qualitative features, but the way in which they fail to do so may well provide information on the underlying physics. In particular, more theoretical attention should be paid to the properties of “clusters” required to explain our data. As mentioned above, Jeon and Shi have proposed that QGP formation would modify the measured properties of clusters [11]. The data shown here should provide means to study such effects, or set upper limits on their occurrence.

This work was partially supported by U.S. DOE grants DE-AC02-98CH10886, DE-FG02-93ER40802, DE-FC02-94ER40818, DE-FG02-94ER40865, DE-FG02-99ER41099, and W-31-109-ENG-38, by U.S. NSF grants 9603486, 0072204, and 0245011, by Polish KBN grant 1-P03B-062-27(2004-2007), by NSC of Taiwan Contract NSC 89-2112-M-008-024, and by Hungarian OTKA grant (F 049823).

-
- [1] R. E. Ansorge *et al.* [UA5 Collaboration], Z. Phys. C **37**, 191 (1988).
 - [2] B. B. Back *et al.* [PHOBOS Collaboration], arXiv:nucl-ex/0301017.
 - [3] B. B. Back *et al.*, Phys. Rev. Lett. **91**, 052303 (2003).
 - [4] K. Alpgard *et al.* [UA5 Collaboration], Phys. Lett. B **123**, 361 (1983).
 - [5] M. Stephanov, K. Rajagopal and E. Shuryak, Phys. Rev. D **60**, 114028 (1999).
 - [6] B. B. Back *et al.* [PHOBOS Collaboration], Nucl. Instrum. Meth. A **499**, 603 (2003).
 - [7] K. Wozniak *et al.* [PHOBOS Collaboration], J. Phys. G **30**, S1377 (2004).
 - [8] Z. Chai, MIT Workshop on Correlations & Fluctuations, Cambridge, MA, April 21-23, Proceedings submitted to IOP.
 - [9] M. Gyulassy and X. N. Wang, Comput. Phys. Commun. **83**, 307 (1994).
 - [10] Z. W. Lin, C. M. Ko, B. A. Li, B. Zhang and S. Pal, Phys. Rev. C **72**, 064901 (2005).
 - [11] L. J. Shi and S. Jeon, Phys. Rev. C **72**, 034904 (2005).

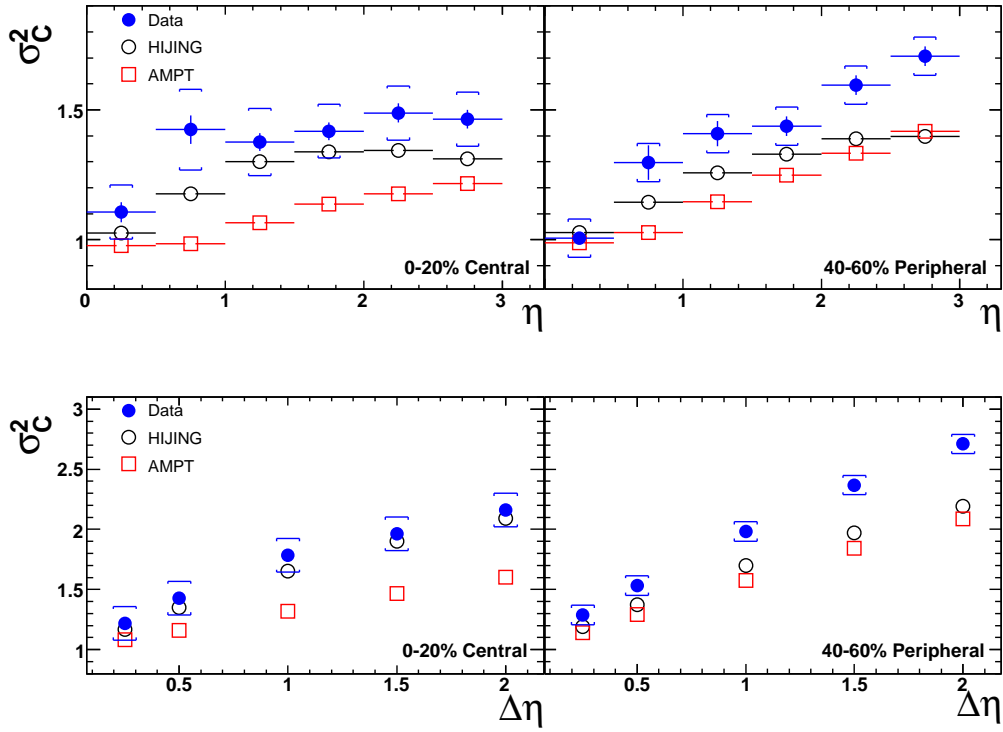


FIG. 5: (upper) σ_C^2 for a fixed $\Delta\eta = 0.5$ as a function of η . (lower) σ_C^2 as a function of $\Delta\eta$ for a fixed bin center at $\eta = 2.0$. Statistical errors are shown as vertical bars, while systematic errors are shown as brackets.